FORCE CAPABILITY MAXIMIZATION OF A 3RRR SYMMETRIC PARALLEL MANIPULATOR BY TOPOLOGY OPTIMIZATION

L. Mejia
Universidade Federal de Santa Catarina, 88040-900 Florianópolis SC Brazil
mejiarinconleonardo@gmail.com

H. Simas
Universidade Federal de Santa Catarina, 88040-900 Florianópolis SC Brazil
hsimas@gmail.com

D. Martins
Universidade Federal de Santa Catarina, 88040-900 Florianópolis SC Brazil
danielemc@gmail.com

Abstract. *This paper shows how the force capability of a 3RRR symmetric parallel manipulator can be maximized from the optimization of its topology. The objective function of the optimization problem of force capability is defined by employing the Screws Theory and Davies's method as a primary mathematical tool. In order to solve the problem regarding the global optimization, an evolutionary algorithm known as Differential Evolution (DE) is used. The proposed method is analysed through specific case studies and evaluated by comparing results versus theoretical methodologies. The key difference from other studies, is that the proposed method allows to optimize the force capability and the topological characteristics of the manipulator at the same time.*

Keywords: *kinematics of position, force capability, trajectory of force, optimization*

1. INTRODUCTION

The increased complexity of the tasks of industrial robots requires further studies on robots interaction with the environment. This interaction can be static, in case there is no relative movement of the robot in relation to the environment, or dynamic, whenever there is this kind of motion, but the contact is maintained during the movement. When movement is slow, it is possible to consider the interaction as quasi-static, because the dynamic effects can be disregarded (Weihmann, 2011), as is the case in the present study .

The task space capabilities of a manipulator to perform motion and/or to exert forces and moments are of fundamental importance in robotics. In the design phase, their evaluation can be useful to determine the structure and the size of a manipulator that best fits the designer's requirements. In the operational phase, they can be used to find a better configuration or a better operation point for a manipulator to perform a given task (Chiacchio *et al.*, 1996).

Industrial robots can be lead to their force capability limit, once are given some specific condition tasks. When performing a task, the force required to accomplish it could exceed the force capability of the robot, and there may be damage or injury (Weihmann, 2011). The main objective of this study is to develop a method to maximize the force capability of a 3RRR symmetrical planar parallel manipulator in static or quasi-static conditions.

In robotics, the force capability of a manipulator is defined as the maximum wrench that can be applied (or sustained) by a manipulator for a given pose based on the limits of the actuators. By considering all possible directions of the applied wrench or by considering specific directions along spatial trajectories, a force capability plot can be generated for the given pose (Nokleby *et al.*, 2004).

The force capability of a manipulator depends on its design, posture and actuation limits(Weihmann *et al.*, 2011). The maximum force with a prescribed moment ($Fapp$)(Firmani *et al.*, 2008) and the maximum available value (MAV) (Finotello *et al.*, 1998) are similar force capabilities performance indices and can be defined as the maximum force that can be applied (or sustained) by a manipulator with a prescribed moment. If this prescribed moment is zero, it yields a pure force analysis. For a given direction, the maximum force that can be applied with zero moment will be denoted as F_m. The scaling factor method and the explicit method to evaluate the force capabilities of parallel manipulators have been presented in (Zibil *et al.*, 2007). Nokleby *et al.* (2007) used those methods to show some results for 3-RRR, 3-RPR and 3-PRR parallel architectures with redundant and non-redundant actuation. Other wrench performance indices for planar parallel manipulators were presented in (Firmani *et al.*, 2008).

The presence of geometric variable parameters in a force optimization problem generates non-linear and non-convex functions over the search space and therefore a global optimization method should be used (Weihmann *et al.*, 2011).

The global optimization problem is not easy to solve and it is still an open challenge for researchers since an analytical optimal solution is difficult to obtain, even for relatively simple application problems. Conventional deterministic

numerical algorithms tend to stop the search in the nearest local minimum to the input starting point, mainly when the optimization problem presents non-linear, non-convex and non-differential functions, multi-modal and non-linear (Weihmann *et al.*, 2011).

Evolutionary algorithms (EAs) are a class of stochastic search and optimization methods, based on the principles of natural biological evolution. In this context, a new EA paradigm, called differential evolution (DE) algorithm, was proposed in (Storn and Price, 2005) and (Storn and Price, 1997). Starting from a population of randomly initialized solutions using uniform distribution, the DE algorithm employs simple mutation and crossover operators to generate new candidate solutions, and utilizes a one-to-one competition scheme to deterministically decide whether the offspring will replace their parents in the next generation. Due to the features of fast convergence and to a few number of control parameters, the DE algorithm, nowadays has emerged as a new and attractive optimizer and applied in different robotic fields (Wang *et al.*, 2008),(Zha, 2002), (Gonzalez *et al.*, 2009).

In this study, *DE* was used to optimize the force capability and the topology of the 3RRR planar manipulator on a given force trajectory in comparison to the approaches in literature.

The remainder of this paper is structured as follows: Section 2 provides a description about geometry, kinematic, and static of the studied manipulator. Section 3 shows and explains the objective function to optimize. Section 4 discusses and presents optimization results and finally, section 5, outlines a brief conclusion about this study.

2. GEOMETRY, KINEMATICS AND STATICS OF THE MANIPULATOR

According to their movement characteristics and mechanical structure, parallel manipulators can be classified into planar, spatial, and spherical (Tsai, 1999). Parallel manipulators usually consist in a mobile platform connected to a fixed platform by several legs in order to transmit the movement. Generally, the number of legs of parallel manipulators is equals to their degree of freedom (DoF), and the motors are usually located near the fixed base (Tsai, 1999).

A parallel manipulators is called symmetrical if it satisfies the following conditions (Mohamed and Duffy, 1985):

1. The number of limbs is equal to the number of DoF of the moving platform.
2. The type and number of joints in all the limbs are arranged in an identical pattern.
3. The number and location of actuated joints in all the limbs are the same.

2.1 Geometry of the manipulator

In this study case, the analysed manipulators are specifically *"3RRR symmetrical planar parallel manipulators"*, that are parallel manipulators which fixed and mobile platforms are joined by using three legs. Each leg has three rotational joints which axes are perpendicular to the $(x-y)$ plane, and the first of the three joints in each leg is actuated. A *"3RRR symmetrical planar parallel manipulator (SPPM)"* is represented schematically in Fig. 1.

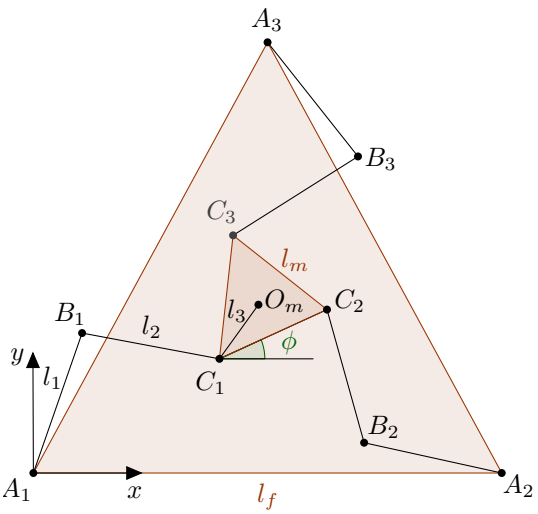

Figure 1. Schematic representation of a SPPM type 3RRR.

As shown in Fig. 1 the mobile and fixed platforms are formed by equilateral triangles with sides l_m and l_f respectively. The legs are formed by two links with longitudes l_1 and l_2 respectively, and the distance between one of the mobile platform vertices and its centroid is called l_3. This distance can be calculated in terms of the distance l_m using Eq. (1). The angle ϕ represents the orientation of the mobile platform.

$$l_3 = \frac{l_m}{2\cos(30°)} \tag{1}$$

Altogether this manipulator is a mechanism with eight links and nine joints, and its mobility can be calculated using the mobility general criterion, as shown in Eq. (2).

$$M = \lambda(n - j - 1) + \sum_{i=1}^{j} f_i = 3(8 - 9 - 1) + 9 = 3 \tag{2}$$

In this mechanism of 3 DoF, the mobile platform is determined as the final effector link, and the l_1 links in the three legs are the inputs links. In this case, the primary actuation is applied to the joints A_1 , A_2 and A_3 of the fixed platform.

2.2 Kinematics of the manipulator

Given the pose (position and orientation) of the mobile platform, the inverse kinematic problem (IKP) consists in finding the corresponding rotation angle or displacement of all joints (active and passive) to achieve this pose. In the absence of kinematics redundancy, each possible solution is known as a different working mode. For instance, the parallel 3-RRR manipulator can operate in eight different working modes (Alba-Gomez *et al.*, 2007).

The inverse kinematic of the manipulator is defined in Eq. (3), Eq. (4) and Eq. (5), and the components C_1, C_2 and C_3 of these equations can be calculated in function of ϕ, l_m and O_m using Eq. (6), Eq. (7) and Eq. (8).

$$\theta_1 = \arctan\left(\frac{C_{1y}}{C_{1x}}\right) \pm \arccos\frac{\sqrt{{C_{1x}}^2 + {C_{1y}}^2}^2 + {l_1}^2 - {l_2}^2}{2l_1\sqrt{{C_{1x}}^2 + {C_{1y}}^2}} \tag{3}$$

$$\theta_2 = \arctan\left(\frac{C_{2y} - A_{2y}}{C_{2x} - A_{2x}}\right) \pm \arccos\frac{\sqrt{(A_{2x} - C_{2x})^2 + (A_{2y} - C_{2y})^2}^2 + {l_1}^2 - {l_2}^2}{2l_1\sqrt{(A_{2x} - C_{2x})^2 + (A_{2y} - C_{2y})^2}} \tag{4}$$

$$\theta_3 = \pi - \arctan\left(\frac{A_{3y} - C_{3y}}{A_{3x} - C_{3x}}\right) \pm \arccos\frac{\sqrt{(A_{3x} - C_{3x})^2 + (A_{3y} - C_{3y})^2}^2 + {l_1}^2 - {l_2}^2}{2l_1\sqrt{(A_{3x} - C_{3x})^2 + (A_{3y} - C_{3y})^2}} \tag{5}$$

Where

$$C_1 = (C_{1x}, C_{1y}) = \left(O_{mx} - \frac{l_m}{3}(\cos(\phi) + \cos(\phi + \frac{\pi}{3})), O_{my} - \frac{l_m}{3}(\sin(\phi) + \sin(\phi + \frac{\pi}{3}))\right) \tag{6}$$

$$C_2 = (C_{2x}, C_{2y}) = (C_1 + l_m\cos(\phi), C_1 + l_m\sin(\phi)) \tag{7}$$

$$C_3 = (C_{3x}, C_{3y}) = \left(C_1 + l_m\cos(\phi + \frac{\pi}{3}), C_1 + l_m\sin(\phi + \frac{\pi}{3})\right) \tag{8}$$

2.3 Statics of the manipulator

In static analysis of manipulators, the goal is to determine the force and moment requirements in the joints. It is possible to apply forces and moments in the mechanism joints to analyse the efforts obtained in the final actuator, or to apply external forces and calculate the necessary forces and moments in the joints to balance these external forces.

The wrenches (force and moments) applied (or sustained) can be represented by the vector $F = [F_x F_y M_z]^T$, where F_x and F_y denotes the force in the directions x and y respectively, and M_z denotes the moment around the z axis. The actuator torques of joints A_1, A_2 and A_3 are respectively τA_1, τA_2 and τA_3, denoted by the vector τ.

Using graph theory and the cut-set law (Cazangi, 2008), it is possible to prove that the net degree of constraint in a $3\underline{R}RR$ manipulator is $C_N = 3$. The manipulator does not have actuation redundancy and knowing the three independent

variables the manipulator is statically solved. The independent and dependent variables used in the optimization problem are respectively the actuator torques and the efforts obtained in the final actuator.

Using the formalism presented in (Davies, 1983), the primary variables are known, and the secondary variables are the unknown variables. Considering the actuation torques as the primary variables, the $\widehat{A}_N$ matrix can be obtained using graph theory, screw theory and Kirchhoff-Davies cutset law (Cazangi, 2008), where $\widehat{A}_N$ is the diagonalized unitary action matrix and V is a vector comprising all the unknown wrenches in the manipulator, as shown in Eq. (9).

$$[\widehat{A}_N]_{21\times 21}\tau_{21\times 1} = V_{21\times 1} \tag{9}$$

The complete manipulators action graph is shown in Fig. 2, where the vertex are the manipulator links and the edges are the joints. Existing wrenches in each joint are represented by the symbol $.

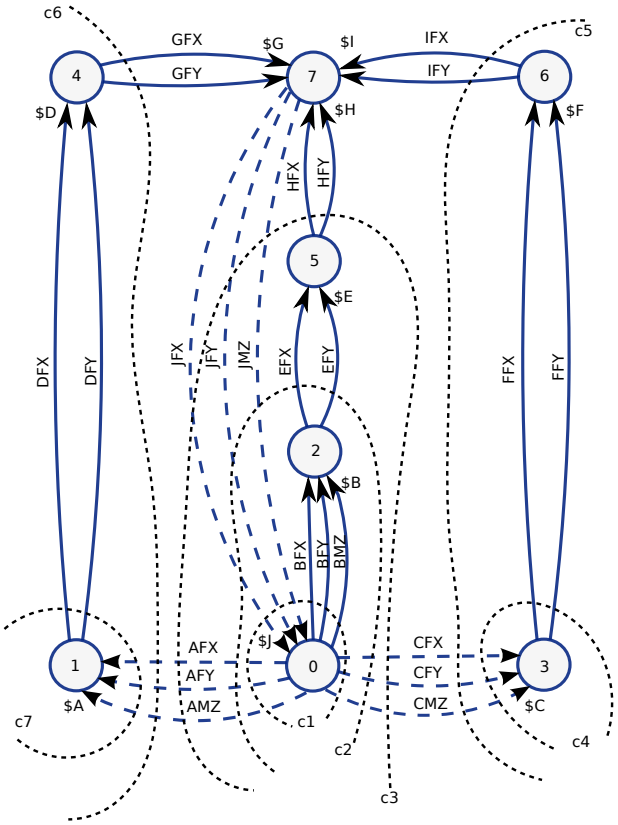

Figure 2. Manipulator action graph of a SPPM type 3RRR

The cutset law states that: when a manipulator is in static equilibrium, the sum of wrenches acting in a single cut must be zero. Each k cut divides the manipulator in subsets of links of joints, where in each subset, the static equilibrium must be preserved (Weihmann *et al.*, 2011).

Since the manipulator is planar, the space dimension λ is three and only the F_x, F_y, and M_z wrench components are considered, while F_z, M_x, and M_y are always equal to zero (Weihmann *et al.*, 2011) and will not be represented in this paper. For revolute joints, the wrench can be written as shown in Eq. (10), where x and y are the location of the joint axis given in Cartesian coordinates, F_x and F_y are respectively the forces in directions x and y, and τ is the actuation torque. If the joint is passive, τ is zero and the last term of equation Eq. (10) vanishes (Weihmann *et al.*, 2011).

$$\$ = \begin{bmatrix} -y \\ 0 \\ 1 \end{bmatrix} F_x + \begin{bmatrix} x \\ 0 \\ 1 \end{bmatrix} F_y + \begin{bmatrix} 1 \\ 0 \\ 0 \end{bmatrix} \tau \tag{10}$$

For each cutset there are three independent equations that can be written in the matrix as shown in Eq. (11).

$$\Sigma\$ = [A_D]_{\lambda\times C} = [\widehat{A}_N]_{\lambda\times C}\{\Psi\}_{C\times 1} = \{0\}_{\lambda\times 1} \tag{11}$$

In in Eq. (11), A_D is the cut action matrix, $\widehat{A}_N$ is the unitary cut action matrix, and Ψ is the vector comprising the wrenches magnitudes. Each column in the A_D matrix represents one wrench that can be separated in a sum of three components. To build the A_D matrix, the following rules must be observed for each cut (Weihmann *et al.*, 2011):

- if a joint is not cut, the columns representing the wrench in this joint are zero.
- if a joint is cut, the wrench is positive or negative regarding the direction assumed for the edge.

Choosing the C_N primary variables, Equation (11) can be manipulated, separating the vector Ψ_p of the primary variables magnitudes from the vector Ψ_s of the secondary variables magnitudes, and the unitary action matrix of the secondary variables $\widehat{A}_{Ns}$ from the unitary action matrix of the primary variables $\widehat{A}_{Np}$, thereby obtaining the Eq. (12), where all wrenches must be written in the same reference frame (Weihmann *et al.*, 2011).

$$\{\Psi\}_{\lambda k\times 1} = [-\widehat{A}_{Ns}^{-1}]_{\lambda k\times\lambda k}[\widehat{A}_{Np}]_{\lambda k\times C_N}\{\Psi_p\}_{C_N\times 1} \tag{12}$$

3. OPTIMIZATION PROBLEM

The main aim of the optimization problem studied in this paper, is to maximize a pure force F_m applied or sustained for the manipulator in a given direction by the angle θ, while the moment is zero or close to zero.

Figure 3 shows the graphic representation of the method used in this paper, where there are two optimization processes involved. The first one, is the optimization process in which the torque in the actuators M_{A1}, M_{A2}, and M_{A3} must be optimized in order to maximize the pure force and minimize the moment in the manipulator's final effector. This optimization must be done in all possible directions given for the angle θ (interval comprehended between $0°$ and $360°$). This process was denoted as "the internal optimization", where were used 360 repetitions in order to represent the 360 different values of the angle θ (interval [0; 360]), and the results were saved in a vector called "Vector of Maximal Forces".

In the second case, the manipulator's topology must be optimized in order to maximize the minimal force obtained in the internal optimization, this was called " the external optimization", where the topological parameters l_1, l_2, and D_2 must be optimized.

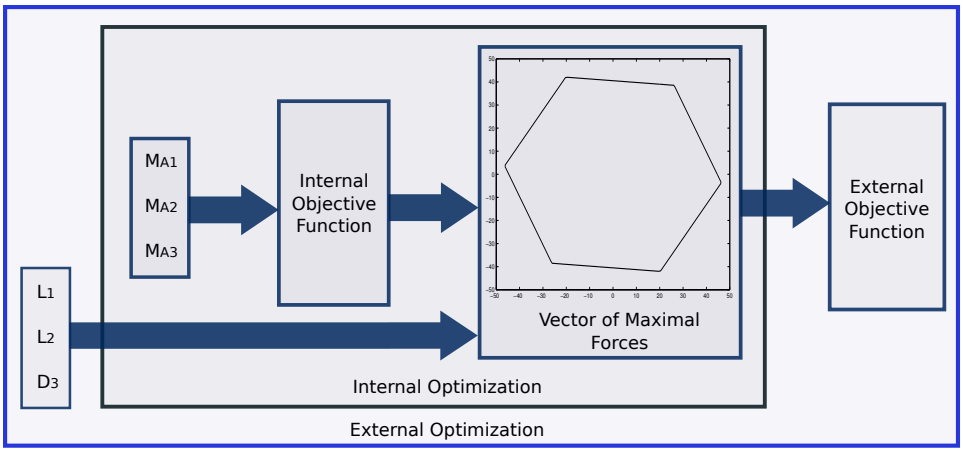

Figure 3. Graphical representation of the proposed optimization

3.1 Objective function and constraints

It is possible to see in Fig. 3 that there are two objective functions. The first one is the "internal Objective Function", that maximizes the force in a given angle and minimizes the moment in the manipulator's final effector. The second one is the "External Objective Function", that maximizes the minimum value saved in the "Vector of Maximal Forces". Thus, the set of forces saved in the "Vector of Maximal Forces" is automatically optimized.

The internal objective function is shown in Eq. (13), where the terms F_x and F_y are the components of the force vector obtained in each iteration of the internal optimization, α_d is the desired angle, α_o is the obtained angle in function of the F_x and F_y components, M_z is the moment obtained in the manipulator's final effector and finally the "PenI" term is the penalization of the internal objective function.

In Eq. (13), the $|\alpha_d - \alpha_o|$ term minimizes the error between the obtained and desired force direction, the $\left|\sqrt{F_x^2 + F_y^2}\right|^{-1}$ term maximizes the force obtained, and the $|M_z|$ term minimizes the moment obtained in the manipulator's final effector

$$F_{obj} = \left(|\alpha_d - \alpha_o| + \frac{1}{\left|\sqrt{F_x^2 + F_y^2}\right|} \right) + (|M_z|) + PenI \tag{13}$$

The external objetive function is shown in Eq. (14), where the term V_{fm} is the "Vector of Maximal Forces" and the "PenE" term is the penalization of the external objective function, here the $(min\,[V_{fm}])^{-1}$ term maximizes the minimum value obtained in the "Vector of Maximal Forces", obtained by the internal optimization for the interval between 0° and 360°.

$$f_{obj2} = \frac{1}{(min\,[V_{fm}])} + PenE \tag{14}$$

The penalization term "PenI" included in Eq. (13) is activated when the condition shown in Eq. (15) is not satisfied (the condition shown in Eq. (15) is imposed as the maximum admissible torque in the actuators), and the penalization term "PenE" included in Eq. (14) is activated when the condition shown in Eq. (16) is not satisfied.

$$-4.2Nm < \tau_{An} < 4.2Nm \tag{15}$$

$$l_1 <= 0, or, l_2 <= 0 \tag{16}$$

As shown in equations Eq. (15) and Eq. (16), the constraints are written in terms of the torque in the actuators τ_{An} and the dimensions of the links l_1 and l_2.

3.2 Diferential Evolution (DE) algorithm

DE is a very simple population based, stochastic function minimizer and very powerful at the same time. This algorithm is commonly accepted as one of the most successful algorithms for the global continuous optimization problem. In fact, it was the best algorithm for the global continuous optimization problem in the first International Contest on Evolutionary Optimization (ICEO).

DE optimizes a problem by maintaining a population of candidate solutions, and creating new candidate solutions by combining existing ones, according to its simple formula, and then keeping whichever candidate solution has the best score or fitness on the optimization problem at hand. In this way, the optimization problem is treated as a black box that merely provides a measure of quality given a candidate solution, and therefore, the gradient is not needed.

The performance of the DE algorithm is sensitive to the mutation strategy and respective control parameters, such as the population size (NP), crossover rate (CR), and the mutation factor (MF). The best settings for control parameters can be different for different optimization problems, and the same functions with different requirements, for consumption time and accuracy (Weihmann *et al.*, 2011).

In this study the parameters $N = 30$, $F = 0.5$, $CR = 0.8$ were used, as suggested in (Storn and Price, 2005), and the maximum iteration number was established in 4000.

4. RESULTS

First of all, the internal optimization was executed using a preset constant topology in order to validate the results obtained in (Nokleby *et al.*, 2004) and (Weihmann *et al.*, 2011). The values used for this optimization are shown below: $l_1 = 0.2m$, $l_2 = 0.2m$, $D_2 = 0.2m$, $O_m x = 0.25m$, $Omy = 0.144m$, and $\phi = 0^\circ$

Varying the θ angle in the interval between 0° and 360°, and optimizing the internal objective function it is possible to find the maximal force applied in each direction of the interval. The result is a force capability hexagon that is exactly equal to the results obtained in (Nokleby *et al.*, 2004). The force capability hexagon is shown in Fig. 4.

In this study, a change in the graphics representation with respect to (Nokleby *et al.*, 2004) is used in order to facilitate the interpretation. This change is shown in Fig. 5, where are plotted the direction of the obtained force (θ in degrees) *Vs* the maximum force obtained in that direction, and the direction of the obtained force (θ in degrees) *Vs* the obtained moment in that direction. (Fig. 4 and Fig. 5 represent basically the same thing).

The behavior of the motors in each optimized point is shown in Fig. 6. And as expected, the results are similar as presented in (Nokleby *et al.*, 2004). The maximal F_M obtained in the interval between 0° and 360° was $46.52N$.

The second case studied, where the whole method is applied, optimizes the topology of the manipulator using the external objective function shown in equation Eq. (14) at the same time that is optimized the manipulator's force capability using the internal objective function shown in equation Eq. (13).

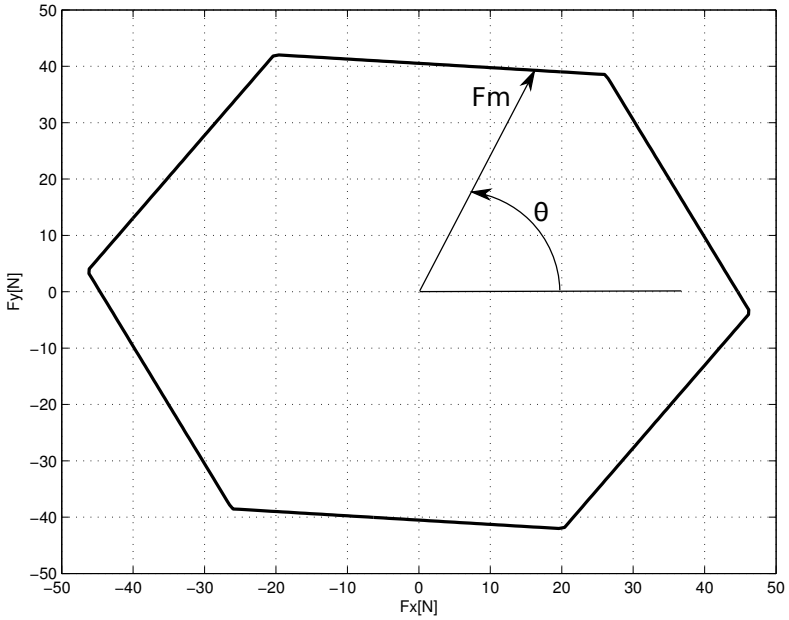

Figure 4. Force capability map

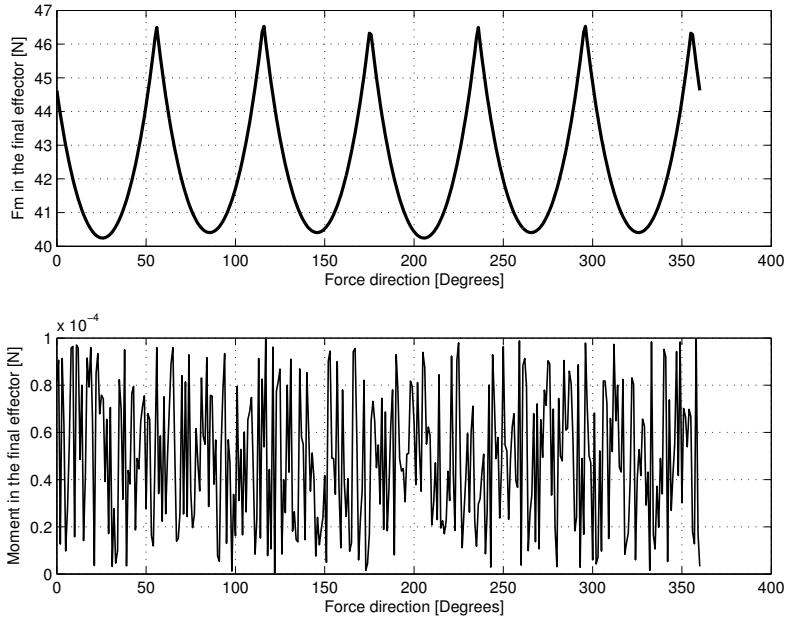

Figure 5. Extended force capability map

Varying the theta angle in the interval between $0°$ and $360°$, and using the propose optimization, the plot shown in Fig. 7 is obtained. The behavior of the motors in each optimized point is shown in the figure Fig. 8.

The results obtained in this last case are better than the results obtained in the first one. The F_M observed is $131.83N$, this implies that the optimized topology offers a maximal force 2.833 times greater than the topology used in the first evaluated case. After the last iteration on the optimization process were obtained the topological values: $l_1 = 0.0621m$ $l_2 = 0.21811m$ and $D_2 = 0.144338m$.

In order to compare, the force capability hexagons obtained in both studied cases are shown on the same graphic, as can be seen in figure Fig. 9, where the hexagon identified with the discontinuous line represents the results obtained in (Nokleby *et al.*, 2004) and (Weihmann *et al.*, 2011), and the hexagon identified with the continuous line represents the results obtained in this study.

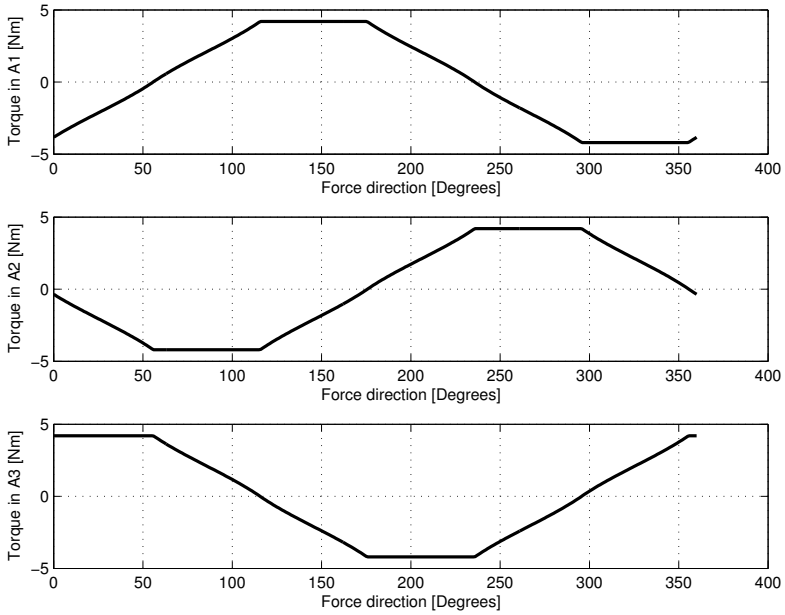

Figure 6. Motor behavior in the force capability

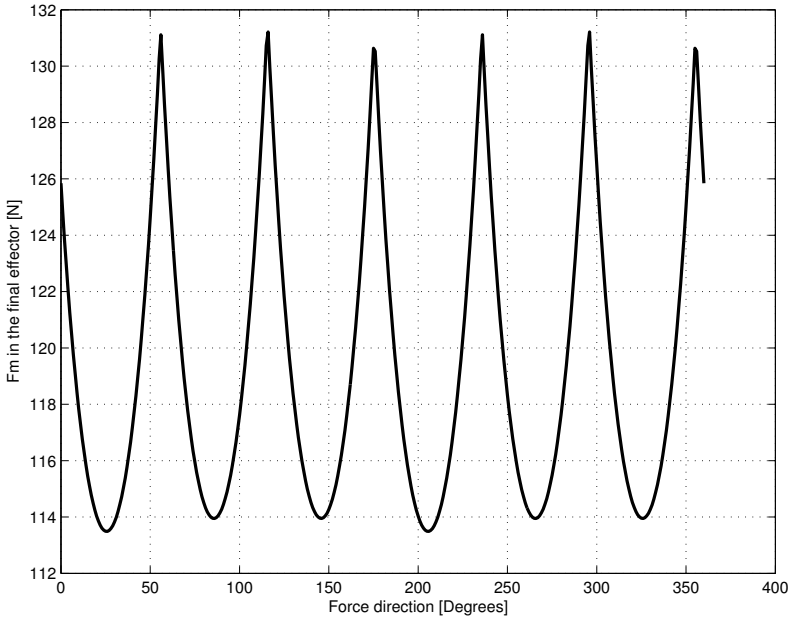

Figure 7. Optimized extended force capability map

5. CONCLUSIONS

This paper presents a new method to optimize the force capabilities in a 3RRR parallel manipulator, optimizing iteratively the torque in the actuators of the manipulator and the topology of the manipulator. The optimization problems were solved using ED algorithms, and the optimization parameters (torque in the actuators and topology) were optimized separately.

Two study cases were shown in order to illustrate the procedure. In the first one, the force capability was maximized by optimization of the torque in the actuators of the manipulator, and in the second one, the force capability was maximized by optimization of both the torque in the actuators of the manipulator and the topology of the manipulator.

As shown in the second study case in this paper, the optimization of the topology of the manipulator allows maximizing the force capabilities using the same torque in the actuators of the manipulator.

Due to the quantity of variables in the topology of the manipulator, the present study may be extended in various ways in order to achieve better force capabilities. In future researches the position and orientation of the mobile platform could be optimized as well as the minimization of the force and the maximization of the moment may be obtained.

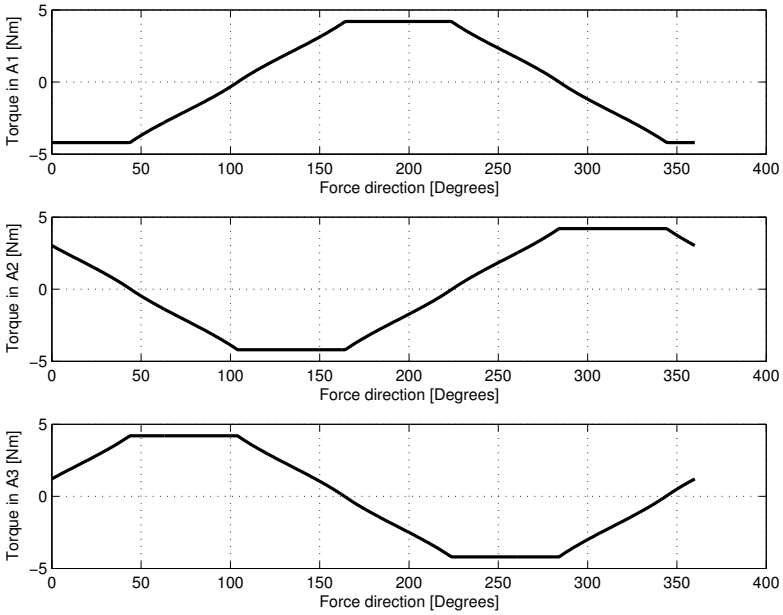

Figure 8. Motor behavior in the optimized extended force capability

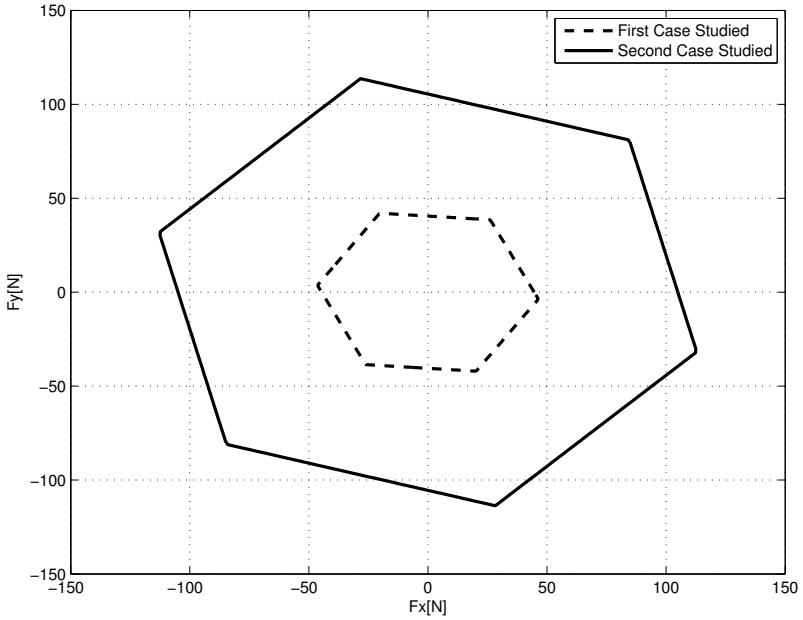

Figure 9. Force capability comparison between the two studied cases

6. ACKNOWLEDGEMENTS

The authors would like to thank CNPq for the partial financial support.

7. REFERENCES

Alba-Gomez, O.G., Pamanes, J.A. and Wenger, P., 2007. "Trajectory planning of a redundant parallel manipulator changing of working mode". *12th IFToMM World Congress on the Theory of Machines and Mechanisms*.

Cazangi, H.R., 2008. *Aplicação do método de Davies para Análise Cinemática e Estática de Mecanismos de Múltiplos Graus de Liberdade*. Ph.D. thesis, Universidade Federal de Santa Catarina, Brazil.

Chiacchio, P., Bouffard-VercelliO, Y. and Pierroto, F., 1996. "Evaluation of force capabilities for redundant manipulators". *IEEE International Conference on Robotics and Automation*, pp. 3520 – 3525.

Davies, T.H., 1983. "Mechanical networks: Wrenches on circuit screws". *Mechanism and Machine Theory*, pp. 107–112.

Finotello, R., Grasso, T., Rossi, G. and Terribile, A., 1998. "Computation of kinetostatic performances of robot manipulators with polytopes". *IEEE International Conference on Robotics and Automation*, pp. 3241 – 3246.

Firmani, F., Zibil, A., Nokleby, S.B. and Podhorodeski, R.P., 2008. "Wrench capabilities of planar parallel manipulators. part i: Wrench polytopes and performance indices". *Robotica 26*, pp. 791 – 802.

Gonzalez, C., Blanco, D. and Moreno, L., 2009. "Optimum robot manipulator path generation using differential evolution". *IEEE Congress on Evolutionary Computation*, pp. 3322–3329.

Mohamed, M.G. and Duffy, J., 1985. "A Direct Determination of the Instantaneous Kinematics of Fully Parallel Robot Manipulators". *Journal of Mechanisms Transmissions and Automation in Design*, Vol. 107. doi:10.1115/1.3258713.

Nokleby, S.B., Firmani, F., Zibil, A. and Podhorodeski, R.P., 2007. "Force moment capabilities of redundantly actuated planar parallel architectures". *12th IFToMM 2007 World Congress*, pp. 17 – 21.

Nokleby, S.B., Fisher, R., Podhorodeski, R.P. and Firmani, F., 2004. "Force capabilities of redundantly-actuated parallel manipulators". *Mechanism and Machine Theory 40*, pp. 578 – 599.

Storn, R. and Price, K., 1997. "Differential evolution : a simple and efficient heuristic for global optimization over continuous spaces". *Journal of Global Optimization*, pp. 341–359.

Storn, R. and Price, K., 2005. "Differential evolution: a simple and efficient adaptive scheme for global optimization over continuous spaces". *Technical Report TR-95-012, International Computer Science Institute*.

Tsai, L.W., 1999. *Robot Analysis and Design: The Mechanics of Serial and Parallel Manipulators*. John Wiley & Sons, Inc., New York, NY, USA, 1st edition. ISBN 0471325937.

Wang, X.S., Hao, M.L. and Cheng, Y.H., 2008. "On the use of differential evolution for forward kinematics of parallel manipulators". *Applied Mathematics and Computation*, pp. 760–769.

Weihmann, L., 2011. *Modelagem e otimização de forças e torques aplicados por robôs com redundância cinemática e de atuação em contato com o meio*. Ph.D. thesis, Universidade Federal de Santa Catarina, Brazil.

Weihmann, L., Martins, D. and Coelho, L.S., 2011. "Force capabilities of kinematically redundant planar parallel manipulators". *13th World Congress in Mechanism and Machine Science*, pp. 483 – 483.

Zha, X.F., 2002. "Optimal pose trajectory planning for robot manipulators". *Mechanism and Machine Theory*, pp. 1063–1086.

Zibil, A., Firmani, F., Nokleby, S.B. and Podhorodeski, R.P., 2007. "An explicit method for determining the force moment capabilities of redundantly actuated planar parallel manipulators". *Mech. Design*, pp. 1046 – 1056.

8. RESPONSIBILITY NOTICE

The authors are the only responsible for the printed material included in this paper.